LncRNA LINC00520 Aggravates Cell Proliferation and Migration in Lung Adenocarcinoma via a Positive Feedback Loop

Wen Huang
The Fourth Affiliated Hospital of Nanjing Medical University
Xinxing Wang
Sir Run Run Hospital of Nanjing Medical University
Fubing Wu (wfbwkx@hotmail.com)
Sir Run Run Hospital of Nanjing Medical University
Fanggui Xu
Sir Run Run Hospital of Nanjing Medical University

Research Article

Keywords: Lung adenocarcinoma, LINC00520, FOXP3, transcription factor, miR-3611

Posted Date: February 24th, 2021

DOI: https://doi.org/10.21203/rs.3.rs-225838/v1

Abstract

Background: Lung adenocarcinoma (LUAD) is the most common histological subtype of primary lung cancer. Thus, to figure out the biomarker of diagnosis for LUAD is of great significance. Long non-coding RNAs (lncRNAs) are previously revealed to exert vital effects in numerous cancers. LncRNA long intergenic non-protein coding RNA 520 (LINC00520) served as an oncogene in certain cancers. Therefore, our report was specially designed to probe role of LINC00520 in LUAD.

Results: LINC00520 expression was detected by RT-qPCR. Next, function of LINC00520 in LUAD was verified by in vitro loss-of-function experiments. As for LINC00520 regulatory mechanism in LUAD, we conducted pull down, ChIP, RIP, and luciferase reporter assays. We found that LINC00520 was upregulated in LUAD. Additionally, LINC00520 upregulation suggested the poorer prognosis for patients with LUAD. Furthermore, LINC00520 downregulation suppressed LUAD cell proliferation and migration and induced cell apoptosis. Simultaneously, forkhead box P3 (FOXP3) is identified as the transcription factor (TF) to transcriptionally activate LINC00520. Moreover, LINC00520 positively upregulated FOXP3 via sponging miR-3611 in LUAD. Subsequently, rescue experiments delineated that miR-3611 downregulation or FOXP3 overexpression could reverse the effect of silenced LINC00520 on proliferative and migratory capabilities in LUAD.

Conclusion: This study first put forward and proved that lncRNA LINC00520 facilitated cell proliferative and migratory abilities in LUAD through interacting with miR-3611 and targeting FOXP3, which may provide a potential novel insight for treatment of LUAD.

Introduction

Lung cancer (LC) is the most common cause of cancer-related death worldwide [1, 2]. The majority of this cancer is non-small-cell lung cancer, of which lung adenocarcinoma (LUAD) is the most common histologic subtype [3, 4], accounting for about 40% of entire lung cancer cases [2]. LUAD remains one of the most aggressive tumor [2, 5], and diagnosed at stages involving proliferation and migration [6, 7]. Despite achievements in its treatment, the prognosis of LUAD patients is still unsatisfied. Thus, it is of great significance to find the biomarker affecting cell proliferation and migration and figure out its regulatory mechanism in LUAD.

With advent of next-generation sequencing, it has now been recognized that most complex eukaryotic genomes are in fact transcribed into noncoding RNAs (ncRNAs), including a family of transcripts with length of over 200 nucleotides regarded as long noncoding RNAs (lncRNAs) [8, 9]. As well known, lncRNAs, functioning as miRNAs sponge, have been characterized in some cancers. And they were involved in regulation in processes such as development and pathologies [10]. For example, AFAP1-AS1 facilitates triple negative breast cancer through sponging miR-145 [11]. LINC00461/miR-30a-5p promotes cell proliferation and migration in NSCLC [12]. Additionally, SPRY4-IT1 accelerates progression of osteosarcoma via interacting with miR-101 [13]. It has been previously reported that lncRNA long intergenic

non-protein coding RNA 520 (LINC00520) served as the tumor promotor in melanoma [14], papillary thyroid carcinoma [15], and colorectal cancer [16], while its role and regulatory mechanism in LUAD remains elusive.

Transcription factors (TFs) are considered to be the main regulators of gene expression [17–19]. Owing to its ubiquitous expression in many tissues, TFs were implicated in extensive biological functions of embryogenesis, cellular proliferation, DNA replication, and differentiation [20]. TFs exert their dual functions - activator or repressor of gene expression, either as activator or repressor [21, 22]. They target specific binding sites to regulate the transcript levels of its downstream genes [23, 24]. Therefore, we wondered which TF could regulate the transcription of LINC00520 in LUAD cells.

In conclusion, our report specially focused on biological role of LINC00520 in LUAD cells. Our data implied that LINC00520 might be a biomarker of treatment for patients with LUAD.

Materials And Methods

Tissue samples

Twenty pairs of LUAD specimens and adjacent non-tumor tissues were acquired from patients who did not receive any therapy before undergoing operation in Sir Run Run Hospital of Nanjing Medical University. Tissue specimens were obtained from patients who signed informed consent. Research was performed in accordance with the Declaration of Helsinki and approval was obtained from the Ethics Committee of the Sir Run Run Hospital of Nanjing Medical University. Immediately after the operation, tissue samples were frozen in liquid nitrogen and maintained at −80 °C.

Cell culture

LUAD cell lines (A549, H1975, H2030, H1435) and a normal human bronchial epithelial cell (BEAS-2B) were provided by the American Type Culture Collection (ATCC; Gaithersburg, MD, USA). Briefly, all cells applied in this study were maintained in Dulbecco's modified Eagle's medium (DMEM; Gibco, Waltham, MA, USA) containing 10% fetal bovine serum (FBS; Gibco, Waltham, MA, USA), 100 U/ml penicillin (Sigma-Aldrich, USA), and 100 mg/ml streptomycin (Sigma-Aldrich, USA) at 37 °C with 5% CO_2.

Cell transfection

To construct pcDNA3.1/LINC00520 or forkhead box P3 (FOXP3) vector, LINC00520 (or FOXP3) were synthesized and subcloned into pcDNA3.1 (Invitrogen, Carlsbad, CA, USA) plasmid. To silence LINC00520, short harpin RNAs (shRNAs) for LINC00520 (sh-LINC00520#1/2), FOXP3 (sh-FOXP3#1/2) and their negative control (sh-NC) were purchased from GenePharma Co., Ltd (Shanghai, China). As for miR-3611, A549 and H1975 cells were transfected with miR-3611 mimics (inhibitor) or NC mimics (inhibitor) by Lipofectamine 2000 (Invitrogen, Carlsbad, CA, USA). MiR-3611 mimics (inhibitor) and NC

mimics (inhibitor) were also supplied by GenePharma (Shanghai, China). A549 and H1975 cells were transfected for 48 h. Additionally, RT-qPCR was applied to testify transfection efficiency.

Real-time quantitative polymerase chain reaction (RT-qPCR)

Total RNA was extracted from frozen tissue samples or cultured cells using Trizol reagent (Thermo Fisher Scientific) and was reverse-transcribed into complementary DNA (cDNA) using a Reverse Transcription Kit (Invitrogen). RT-qPCR analysis was conducted with SYBR Green Premix PCR Master Mix (Roche, Mannheim, Germany) by an ABI HT9600 (Applied Biosystems, Foster City, CA, USA). Glyceraldehyde-3-phosphate dehydrogenase (GAPDH) was taken as the internal reference for LINC00520 and FOXP3. RNU6 (U6) was taken as the internal reference for miR-3611. The $2^{-\triangle\triangle CT}$ method was utilized to calculate the relative quantification.

CCK-8 assay

After transfection, cell viability was measured by Cell Counting Kit-8 (CCK-8; Dojindo, Kyushu, Japan) under the manufacturer's guidance. A549 or H1975 cells (1×10^3) were plated into 96-well plates for 0, 1, 2, and 3 days. CCK- 8 solution was added into plates to cultivate cells for 2 h at 37 °C. Optical density at a wavelength of 450 nm was measured by a microplate reader (Thermo Fisher Scientific).

Colony formation assay

A549 or H1975 cells (1×10^3) were plated into 6-well plates at 37 °C with 5% CO_2. After 2 weeks, colonies were fixed by 4% paraformaldehyde (Solarbio, Beijing, China) for 10 min, and dyed by crystal violet (Beyotime, Nantong, China) for 5 min when colonies were visible. The plates were photographed, and the number of colonies was counted.

Flow cytometry analysis

Transfected cells were collected and resuspended with phosphate buffered saline (PBS). After being cultured at 6-well plates for 48 h, A549 or H1975 cells were fixed in 70% ethanol pre-cooled with ice for 2 h. Quantification of apoptosis was measured by flow cytometry (Thermo Fisher Scientific) after staining with Annexin V-FITC/PI (BD Biosciences, San Jose, CA, USA).

Wound healing assay

After transfection, A549 or H1975 cells seeded in 6-well plates were subjected to serum starvation for 4 h. Thereafter, the wound was stimulated by straight scratching in the cell monolayer using a sterile 200-μl

pipette tip. After gently scraping the scratched monolayer cells twice with serum-free medium, the wound was healed in complete medium for 24 h. Then, after the wound was formed, photographs of the wound width at 0 and 24 h were captured using an inverted microscope, respectively. LUAD cell migration was assessed by checking the percentage of wound closure.

Western bolt

Cells were lysed with lysis buffer containing protease inhibitors (50 mM Tris-HCl pH 8; 50 mM NaCl; 0.5% NP-40). Total protein was extracted from tissues and cells using radioimmunoprecipitation assay buffer (Thermo Fisher Scientific, Inc.). Protein concentration was determined using a bicinchoninic acid assay. The extracted total protein (20 μg) was subjected to 10% sodium dodecyl sulfate-polyacrylamide gel electrophoresis (SDS-PAGE; Solarbio, Beijing, China) and transferred to polyvinylidene fluoride (PVDF) membranes (Sigma-Aldrich, Shanghai, China). After PVDF membranes was blocked with 5% skim milk at 25°C for 1 h, the primary antibodies were added for incubation overnight, including anti-E-cadherin (Abcam), anti-N-cadherin (Abcam) and anti-GAPDH (Abcam). After adding secondary antibody, proteins were visualized by an enhanced chemiluminescence detection kit (Amersham Pharmacia Biotech, UK) and a Bio-Rad image analysis system (Bio-Rad, CA, USA).

DNA pull down

A DNA pull-down test kit (Gzscbio, Guangzhou, China) was utilized under manufacturer's guidance. Biotin-labeled promoter bound with streptavidin magnetic beads were cultivated with cellular protein extracts at 4 °C overnight, and separated by SDS-PAGE, detected by RT-qPCR.

Chromatin immunoprecipitation (ChIP) assay

A chromatin immunoprecipitation (ChIP) assay was carried out with the Magna ChIP Kit (Millipore, Billerica, MA) under manufacturer's instruction. The following antibodies were utilized to immunoprecipitated crosslinked protein-DNA complexes prior to RT-qPCR analysis using rabbit anti-FOXP3 and normal rabbit IgG.

Luciferase reporter assay

The wild-type plasmids of FOXP3 3'UTR containing the putative binding site of miR-3611 and their mutations were cloned into the pmiRGLO dual-luciferase vector (Promega, Madison, WI, USA), termed FOXP3-WT/MUT. The plasmids were co-transfected with indicated plasmids into A549 or H1975 cells with Lipofectamine 2000 (Invitrogen). The promoter sequences of LINC00520 were subcloned into pGL3 luciferase vector to construct promoter luciferase plasmids, and then co-transfected with indicated

plasmids into A549 or H1975 cells. Dual-Luciferase Reporter Assay System (Promega) was utilized to confirm Luciferase activities.

Subcellular fractionation

The cytoplasmic and nuclear extracts were extracted from A549 or H1975 cells by Nuclear and Cytoplasmic Extraction Reagents (Thermo Fisher Scientific). RNAs isolated from nucleus or cytoplasm were performed RT-qPCR analysis. The levels of U6 (nucleus control), GAPDH (cytoplasm control), and LINC00520 were respectively determined.

RNA immunoprecipitation (RIP) assay

RNA immunoprecipitation (RIP) experiment was conducted through the Magna RIP™ RNA-Binding Protein Immunoprecipitation Kit (Millipore, Billerica, MA) under manufacturer's instruction. Ago2 antibody was applied for RIP (Cell Signaling Technology, Beverly, MA). RT-qPCR was utilized to detect co-precipitated RNAs. IgG controls were assayed simultaneously to demonstrate that the detected signals were the result of RNAs specifically binding to Ago2.

Statistical analysis

Data of triplicate experiments were analyzed by SPSS (SPSS Inc., Chicago, IL, USA). Results acquired were denoted as means ± standard deviation (SD). Kaplan Meier and Log-rank test were performed for survival curve. Comparison between two groups was evaluated by Student's t test or comparison among three groups was assessed with analysis of variance (ANOVA) followed by Turkey's post-hoc test. Each experiment was repeated three times in triplicate. $p < 0.05$ was considered as statistically differential significance.

Results

LINC00520 was upregulated in LUAD and facilitated cell proliferation and migration in LUAD

Under RT-qPCR result, LINC00520 presented upregulation in LUAD tissues than in adjacent non-tumor ones (Fig. 1A). In addition, LINC00520 expression was higher in LUAD cells (A549, H1975, H2030, H1435) compared to normal cell line (BEAS-2B) (Fig. 1B). In addition, we found from Kaplan Meier analysis that LINC00520 upregulation implied unfavorable prognosis of patients with LUAD (Fig. 1C). Subsequently, some loss-of-function experiments validated LINC00520 biological function in LUAD. First, we knocked down LINC00520 with sh-LINC00520 plasmids and sh-NC was utilized as scramble control. LINC00520 expression under sh-LINC00520 was downregulated in LUAD cells compared with in scramble control

group (Fig. 1D). Proliferation of A549 and H1975 cells was confirmed with CCK-8 and colony formation experiments. As a result, LINC00520 silencing repressed cell viability and number of colonies, indicating that LINC00520 silencing impeded LUAD cell proliferation (Fig. 1E and Fig. 1F). Furthermore, it was depicted that LINC00520 knockdown accelerated the apoptosis of LUAD cells (Fig. 1G-H). Moreover, the migratory ability of LUAD cells was abolished by LINC00520 depletion (Fig. 1I). In parallel, EMT process in LUAD was determined via measuring EMT marker levels. Through western blot experiments, we found that E-cadherin level showed a significant increase, and N-cadherin level showed a significant decrease under LINC00520 depletion (Fig. 1I and Fig. 1J).

FOXP3 transcriptionally induced upregulation of LINC00520 in LUAD cells

Then, we explored mechanism about LINC00520 upregulation in LUAD cells. As well known, dynamic interaction of TFs with degenerate DNA pattern on promoters leads to activation of certain oncogenes in cancers. Therefore, we wondered whether LINC00520 was activated by TF in LUAD. Through UCSC and PROMO, we predicted 22 potential TFs (condition: within a dissimilarity margin less or equal than 0%) bound to promoters of LINC00520 (Fig. 2A). To probe interaction between TFs and LINC00520 promoter, DNA pull down assay was conducted. Results revealed that three TFs (FOXP3, YY1 and XBP-1) showed enrichment in LINC00520 promoter sense group than in antisense group (Fig. 2B). Simultaneously, RT-qPCR was utilized to measure expression of three TFs in LUAD cells and normal ones. As presented in Fig. 2C, FOXP3 was upregulated in LUAD cells, and the other two TFs were not. Additionally, FOXP3 illustrated the upregulation in LUAD tissues rather than in adjacent non-tumor ones (Fig. 2D). Therefore, FOXP3 was proved to be the transcriptional activator of LINC00520 upregulation in LUAD. Subsequently, to detect FOXP3 effect on LINC00520 expression, we transfected FOXP3 with pcDNA3.1/FOXP3 or sh-FOXP3#1/2 (Fig. 2E). Consequently, we found that FOXP3 overexpression upregulated LINC00520 expression and FOXP3 silencing downregulated LINC00520 expression in LUAD cells (Fig. 2F). Through JASPAR database, 5 potential binding sites of FOXP3 were predicted for LINC00520 at the promoter region (condition: threshold value greater than 90) (Fig. 2G). In parallel, ChIP experiment validated that DNA sequence which contained site 5 showed an enrichment in FOXP3 immunoprecipitation product (Fig. 2H), which suggested abundant binding with LINC00520 promoter at site 5. Additionally, it was found from luciferase reporter assay that FOXP3 knockdown induced an increase in promoter luciferase activity (Fig. 2I).

LINC00520 interacted with miR-3611 to regulate FOXP3

Subsequently, we investigated regulatory mode of LINC00520 on FOXP3. As FOXP3 transcriptionally activated LINC00520, we wondered whether LINC00520 regulated FOXP3 expression in turn. Under RT-qPCR analysis, LINC00520 knockdown suppressed FOXP3 expression and LINC00520 upregulation increased FOXP3 expression (Fig. 3A and Fig. 3B). It suggested that LINC00520 positively modulated

FOXP3. We thus wondered the regulatory mechanism of LINC00520 on FOXP3. Next, subcellular fractionation experiment revealed the cytoplasmic localization of LINC00520 in A549 and H1975 cells (Fig. 3C), indicating post-transcriptional regulation of LINC00520 on downstream genes. It has been reported that lncRNA, located in cytoplasm of cells, served as the competing endogenous RNA (ceRNA). Therefore, we tried to investigate whether LINC00520 could modulate FOXP3 through acted as a ceRNA. Then, the shared miRNA for LINC00520 and FOXP3 was predicted by online tool DIANA and miRDB. As shown by the Venn pattern in Fig. 3D, there were three putative shared miRNAs for LINC00520 and FOXP3. Moreover, three miRNA expression was testified by RT-qPCR in 4 LUAD cells and BEAS-2B cell line. As a result, only miR-3611 was downregulated in LUAD cells (Fig. 3E). Therefore, miR-3611 was identified as a potential shared miRNA for LINC00520. Additionally, it was demonstrated from RT-qPCR result that miR-3611 presented downregulation in LUAD tissues rather than in adjacent non-tumor ones (Fig. 3F). In parallel, we overexpressed miR-3611 with miR-3611 mimics and NC mimics was used as negative control. And it turned out that miR-3611 expression was increased in miR-3611 mimics group (Fig. 3G). Additionally, miR-3611 binding fragment on LINC00520 or FOXP3 was respectively predicted with DIANA and TargetScan as shown in Fig. 3H. Luciferase reporter assay indicated that upregulation of LINC00520 reversed luciferase activity of FOXP3-WT suppressed under miR-3611 overexpression, and FOXP3-Mut presented no significant alteration (Fig. 3I). Simultaneously, through RIP assay, miR-3611 was co-immunoprecipitated with LINC00520 and FOXP3 by Ago2, which revealed that miR-3611 bound to LINC00520 and FOXP3 in RNA-induced silencing complex (RISC) (Fig. 3J).

LINC00520 functioned to be an oncogene in LUAD cells though positive feedback loop of LINC00520/miR-3611/FOXP3

To explore whether LINC00520 modulated cell proliferation and migration by the miR-3611/FOXP3 axis, we performed some rescue experiments as follows. First, it was verified that miR-3611 expression was declined under miR-3611 knockdown (Fig. 4A). Next, inhibitory effect of LINC00520 silencing on viability of A549 cells were abolished under miR-3611 downregulation or FOXP3 upregulation (Fig. 4B). Additionally, pcDNA3.1/FOXP3 or miR-3611 inhibitor rescued the LINC00520-downregulation-mediated decrease in number of colonies (Fig. 4C-D). Furthermore, increased apoptosis of A549 cells caused by LINC00520 silencing was countervailed by miR-3611 downregulation or FOXP3 upregulation (Fig. 4E-F). Additionally, miR-3611 knockdown orFOXP3 overexpression reversed the migratory ability of LUAD cells suppressed by LINC00520 depletion (Fig. 4G). Moreover, the increase in E-cadherin and decrease in N-cadherin under LINC00520-knockdown-mediation was rescued with miR-3611 depletion or FOXP3 elevation (Fig. 4H).

Discussion

Recently, lncRNAs have been found to function as an oncogene in modulating cell proliferation and migration [25, 26]. As previously reported, LINC00520 has an oncogenic effect on melanoma [14], papillary thyroid carcinoma [15], and colorectal cancer [16]. In our report, we first put forward evidence that LINC00520 expression was upregulated in LUAD cells and tissues. Kaplan Meier analysis showed that higher LINC00520 expression in LUAD patients implied poorer prognosis. Functionally, we proved that silenced LINC00520 attenuated proliferative and migratory abilities and promoted apoptosis in LUAD. These results revealed that LINC00520 functioned as an oncogene in LUAD. More and more evidences show that transcriptional activation of lncRNA is mainly responsible for regulation on cancers [27, 28]. Therefore, we wondered the TF by which LINC00520 was activated. As reported, FOXP3 is a forkhead lineage-transcription factor and presented abnormal expression in cancers [29]. As a series of mechanism experiments carried out, we identified that FOXP3 was a TF for transcription of LINC00520.

In our report, we found FOXP3 expression could be positively modulated by LINC00520. In addition, results from subcellular fractionation assay suggested cytoplasmic localization of LINC00520 in LUAD. It implied that LINC00520 post-transcriptionally modulate its downstream gene. Additionally, previous studies have revealed that interactions in ceRNA networks contribute to disease pathogenesis, especially in cancers [30, 31]. Multiple reports illustrated that lncRNA, acted as a ceRNA, regulate downstream gene via sequestering miRNA at post-transcription level. Through bioinformatics, we obtained a newly-identified miRNA - miR-3611. Subsequently, mechanism experiments validated that miR-3611 was the shared miRNA for LINC0020 and FOXP3. Additionally, we confirmed that LINC00520 upregulated FOXP3 by functioning as miR-3611 sponge. In parallel, a series of rescue assays further validated that LINC00520 aggravated LUAD cell proliferation and migration via sponging miR-3611 and targeting FOXP3.

In conclusion, LINC00520 was an oncogenic gene in LUAD and LINC00520 induced proliferation and migration and suppressed apoptosis in LUAD cells. Mechanistically, we revealed that LINC00520 was transcriptionally activated by FOXP3. Moreover, the LINC00520/miR-3611/ FOXP3 positive feedback loop induced proliferation and migration in LUAD cells. Our study potentially provide a new vision for treatment of LUAD.

Declarations

Ethics approval and consent to participate

Research was performed in accordance with the Declaration of Helsinki and approval was obtained from the Ethics Committee of the Sir Run Run Hospital of Nanjing Medical University. Tissue specimens were obtained from patients who signed informed consent.

Consent for publication

Not applicable

Acknowledgements

Thank you for all lab members involved in this study.

Conflict of interest

The authors declare that there exists no conflict of interest.

Availability of data and materials

The datasets used and/or analysed during the current study available from the corresponding author on reasonable request.

Funding

Not applicable

Authors' contributions

Wen Huang and Xinxing Wang carried out the experiments. Wen Huang, Fubing Wu , Fanggui Xu and Xinxing Wang analyzed the data. Wen Huang, Xinxing Wang, Fubing Wu and Fanggui Xu drafted the manuscript. All authors agreed to be accountable for all aspects of the work. All authors have read and approved the final manuscript.

References

1. Cheung CHY and Juan HF. Quantitative proteomics in lung cancer. *Journal of biomedical science*. 2017; 24: 37.
2. Bodor JN, Kasireddy V and Borghaei H. First-Line Therapies for Metastatic Lung Adenocarcinoma Without a Driver Mutation. *Journal of oncology practice*. 2018; 14: 529-35.
3. Hutchinson BD, Shroff GS, Truong MT and Ko JP. Spectrum of Lung Adenocarcinoma. *Seminars in ultrasound, CT, and MR*. 2019; 40: 255-64.
4. Balzer BWR, Loo C, Lewis CR, Trahair TN and Anazodo AC. Adenocarcinoma of the Lung in Childhood and Adolescence: A Systematic Review. *Journal of thoracic oncology : official publication of the International Association for the Study of Lung Cancer*. 2018; 13: 1832-41.
5. Jiang N and Xu X. Exploring the survival prognosis of lung adenocarcinoma based on the cancer genome atlas database using artificial neural network. *Medicine*. 2019; 98: e15642.

6. Suber TL, Nikolli I, O'Brien ME, et al. FBXO17 promotes cell proliferation through activation of Akt in lung adenocarcinoma cells. *Respiratory research*. 2018; 19: 206.
7. Ko PH, Lenka G, Chen YA, et al. Semaphorin 5A suppresses the proliferation and migration of lung adenocarcinoma cells. *International journal of oncology*. 2020; 56: 165-77.
8. Charles Richard JL and Eichhorn PJA. Platforms for Investigating LncRNA Functions. *SLAS technology*. 2018; 23: 493-506.
9. Paraskevopoulou MD and Hatzigeorgiou AG. Analyzing MiRNA-LncRNA Interactions. *Methods in molecular biology (Clifton, NJ)*. 2016; 1402: 271-86.
10. Jarroux J, Morillon A and Pinskaya M. History, Discovery, and Classification of lncRNAs. *Advances in experimental medicine and biology*. 2017; 1008: 1-46.
11. Zhang X, Zhou Y, Mao F, Lin Y, Shen S and Sun Q. lncRNA AFAP1-AS1 promotes triple negative breast cancer cell proliferation and invasion via targeting miR-145 to regulate MTH1 expression. *Scientific reports*. 2020; 10: 7662.
12. Li X, Liu J, Liu M, Xia C and Zhao Q. The Lnc LINC00461/miR-30a-5p facilitates progression and malignancy in non-small cell lung cancer via regulating ZEB2. *Cell cycle (Georgetown, Tex)*. 2020; 19: 825-36.
13. Yao H, Hou G, Wang QY, Xu WB, Zhao HQ and Xu YC. LncRNA SPRY4-IT1 promotes progression of osteosarcoma by regulating ZEB1 and ZEB2 expression through sponging of miR-101 activity. *International journal of oncology*. 2020; 56: 85-100.
14. Luan W, Ding Y, Yuan H, et al. Long non-coding RNA LINC00520 promotes the proliferation and metastasis of malignant melanoma by inducing the miR-125b-5p/EIF5A2 axis. *Journal of experimental & clinical cancer research : CR*. 2020; 39: 96.
15. Sun Y, Shi T, Ma Y, Qin H and Li K. Long noncoding RNA LINC00520 accelerates progression of papillary thyroid carcinoma by serving as a competing endogenous RNA of microRNA-577 to increase Sphk2 expression. *Cell cycle (Georgetown, Tex)*. 2020; 19: 787-800.
16. Jin XH, Hong YG, Li P, Hao LQ and Chen M. Long noncoding RNA LINC00520 accelerates the progression of colorectal cancer by serving as a competing endogenous RNA of microRNA-577 to increase HSP27 expression. *Human cell*. 2020.
17. Khazaei N, Rastegar-Pouyani S, O'Toole N, Wee P, Mohammadnia A and Yaqubi M. Regulating the transcriptomes that mediate the conversion of fibroblasts to various nervous system neural cell types. *Journal of cellular physiology*. 2018; 233: 3603-14.
18. Perez-Rueda E, Hernandez-Guerrero R, Martinez-Nuñez MA, Armenta-Medina D, Sanchez I and Ibarra JA. Abundance, diversity and domain architecture variability in prokaryotic DNA-binding transcription factors. *PloS one*. 2018; 13: e0195332.
19. Mahdevar G, Sadeghi M and Nowzari-Dalini A. Transcription factor binding sites detection by using alignment-based approach. *Journal of theoretical biology*. 2012; 304: 96-102.
20. Ustiyan V, Bolte C, Zhang Y, et al. FOXF1 transcription factor promotes lung morphogenesis by inducing cellular proliferation in fetal lung mesenchyme. *Developmental biology*. 2018; 443: 50-63.

21. Kim JG and Mudgett MB. Tomato bHLH132 Transcription Factor Controls Growth and Defense and Is Activated by Xanthomonas euvesicatoria Effector XopD During Pathogenesis. *Molecular plant-microbe interactions : MPMI*. 2019; 32: 1614-22.
22. Narayan S, Bryant G, Shah S, Berrozpe G and Ptashne M. OCT4 and SOX2 Work as Transcriptional Activators in Reprogramming Human Fibroblasts. *Cell reports*. 2017; 20: 1585-96.
23. Yu CP and Li WH. Predicting Transcription Factor Binding Sites and Their Cognate Transcription Factors Using Gene Expression Data. *Methods in molecular biology (Clifton, NJ)*. 2017; 1629: 271-82.
24. Crocker J, Noon EP and Stern DL. The Soft Touch: Low-Affinity Transcription Factor Binding Sites in Development and Evolution. *Current topics in developmental biology*. 2016; 117: 455-69.
25. Sanchez Calle A, Kawamura Y, Yamamoto Y, Takeshita F and Ochiya T. Emerging roles of long non-coding RNA in cancer. *Cancer science*. 2018; 109: 2093-100.
26. Ulitsky I and Bartel DP. lincRNAs: genomics, evolution, and mechanisms. *Cell*. 2013; 154: 26-46.
27. Chen JF, Wu P, Xia R, et al. STAT3-induced lncRNA HAGLROS overexpression contributes to the malignant progression of gastric cancer cells via mTOR signal-mediated inhibition of autophagy. *Molecular cancer*. 2018; 17: 6.
28. Chen X, Zeng K, Xu M, et al. SP1-induced lncRNA-ZFAS1 contributes to colorectal cancer progression via the miR-150-5p/VEGFA axis. *Cell death & disease*. 2018; 9: 982.
29. Vadasz Z and Toubi E. FoxP3 Expression in Macrophages, Cancer, and B Cells-Is It Real? *Clinical reviews in allergy & immunology*. 2017; 52: 364-72.
30. Karreth FA and Pandolfi PP. ceRNA cross-talk in cancer: when ce-bling rivalries go awry. *Cancer discovery*. 2013; 3: 1113-21.
31. Smillie CL, Sirey T and Ponting CP. Complexities of post-transcriptional regulation and the modeling of ceRNA crosstalk. *Critical reviews in biochemistry and molecular biology*. 2018; 53: 231-45.

Figures

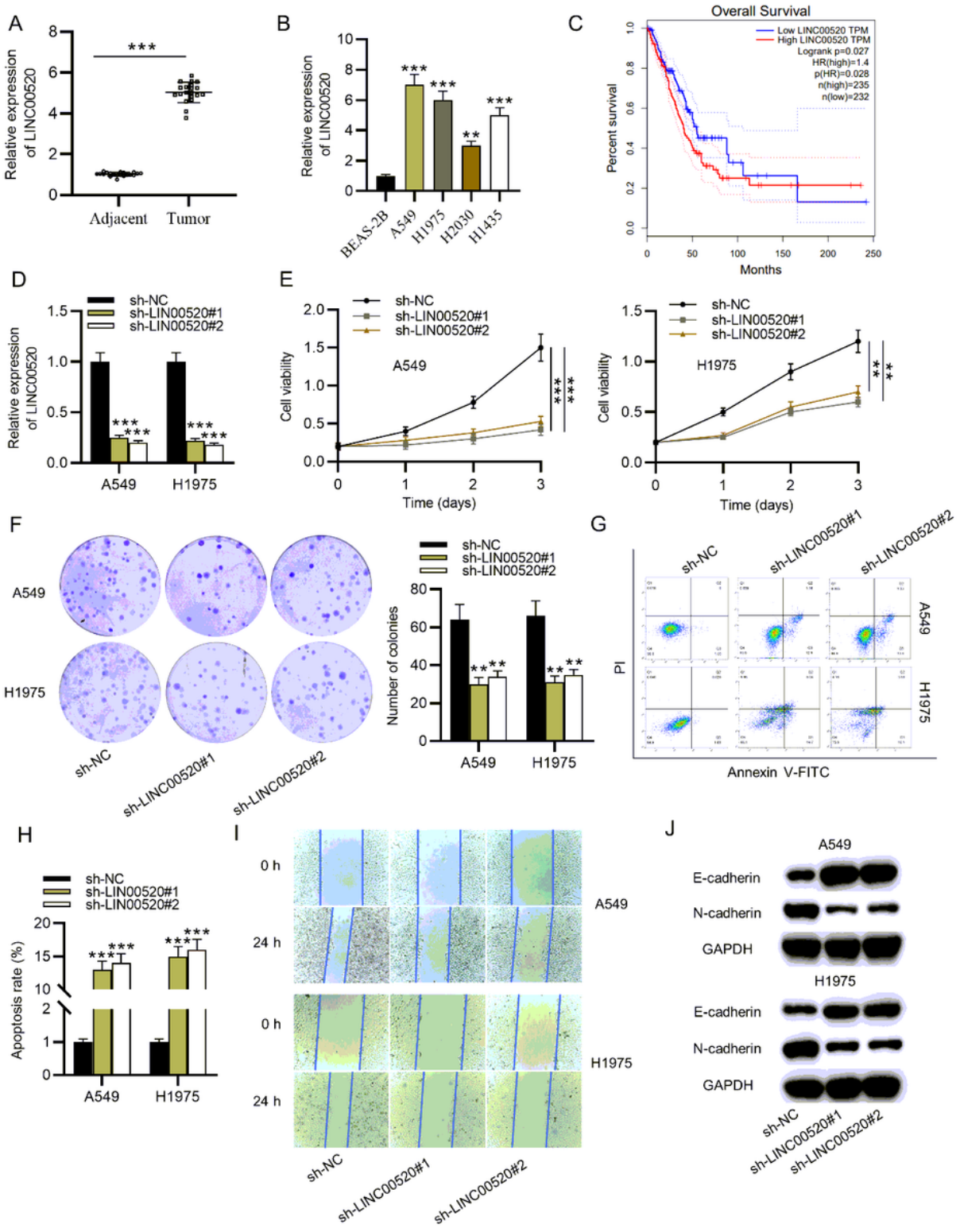

Figure 1

LINC00520 presented upregulation in LUAD and aggravated proliferation and migration in LUAD cells. (A) LINC00520 level in LUAD tissues and adjacent non-tumor ones was examined through RT-qPCR. (B) RT-qPCR testified LINC00520 expression in 4 LUAD cells and BEAS-2B cell line. (C) Kaplan Meier analysis depicted the survival curve for prognosis of patients with LUAD. (D) RT-qPCR detected knockdown efficacy of sh-LINC00520#1/2 in LUAD cells. (E) CCK-8 assay was adopted to confirm viability of LUAD

cells under LINC00520 silencing. (F) Colony formation assay assessed LUAD cell proliferation affected by LINC00520 knockdown. (G-H) Cell apoptosis in LUAD influenced by LINC00520 downregulation was analyzed by flow cytometric analysis. (I) Migrative ability of LUAD cells was verified with wound healing experiment after LINC00520 downregulation. (J) Western blot analysis examined protein expression levels of EMT markers affected by LINC00520 silencing. **p < 0.01, ***p < 0.001.

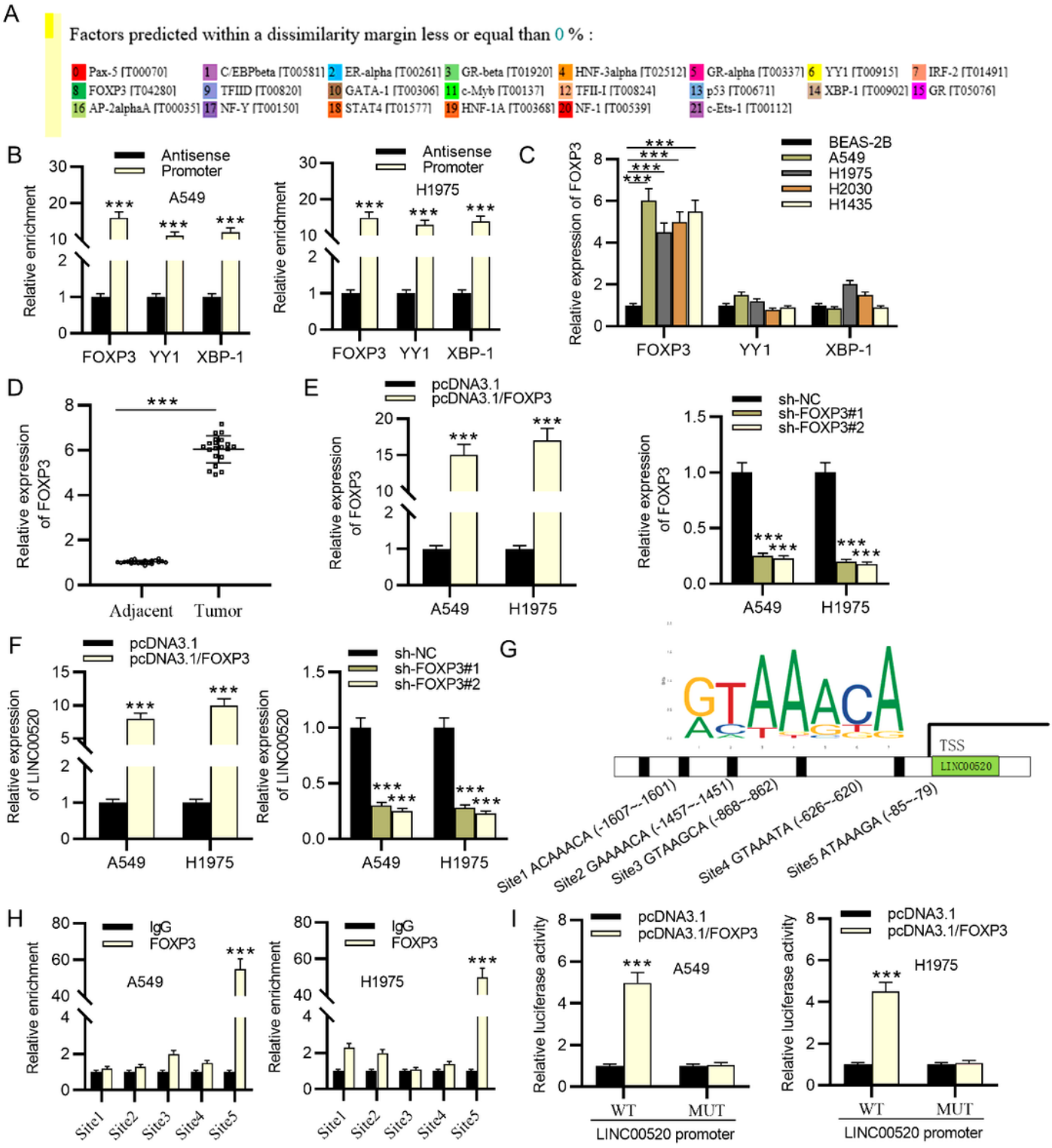

Figure 2

FOXP3 transcriptionally activated LINC00520 in LUAD cells. (A) TFs for LINC00520 promoter were predicted though online tool UCSC and PROMO. (B) Binding effects between putative TFs and LINC00520 promoter were illustrated by pull down assay. (C) RT-qPCR analysis confirmed expression of putative TFs in LUAD. (D) RT-qPCR testified FOXP3 levels in LUAD tissues and adjacent non-tumor ones. (E) The transfection efficiency of pcDNA3.1/FOXP3 or sh-FOXP3#1/2 in LUAD cells was determined by RT-qPCR. (F) Effects of sh-FOXP3#1/2 and pcDNA3.1/FOXP3 on LINC00520 were confirmed by RT-qPCR. (G) Five FOXP3 binding sites on LINC00520 promoter were predicted through online tool JASPAR. (H) ChIP assay presented FOXP3 binding site of LINC00520 promoter. (I) Luciferase reporter assay validated the effect of FOXP3 overexpression on luciferase activity of LINC00520 promoter-WT/MUT vector. ***$p < 0.001$.

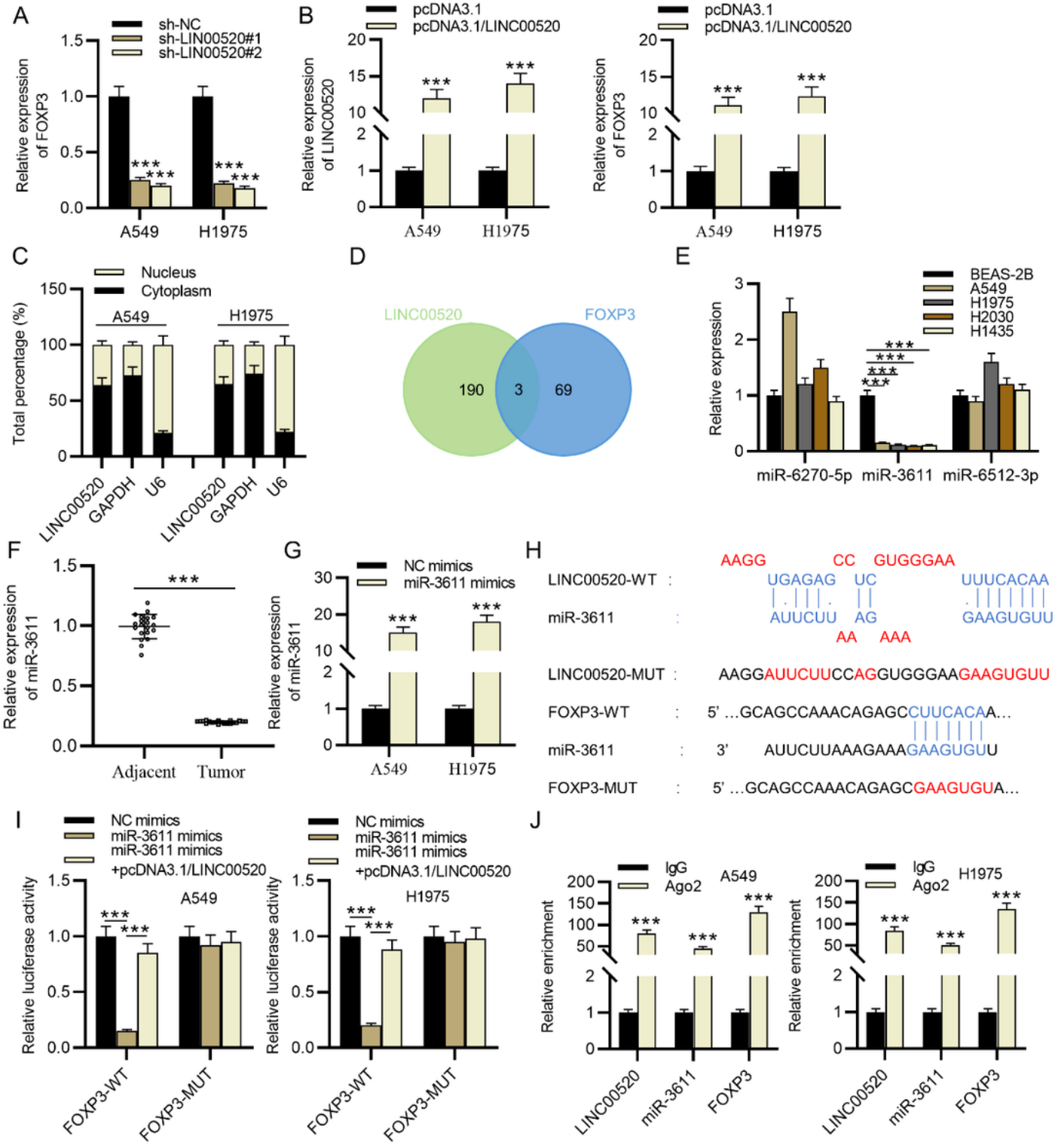

Figure 3

LINC00520 upregulated FOXP3 expression by binding to miR-3611. (A) Effect of sh-LINC00520#1/2 on FOXP3 expression was testified with RT-qPCR. (B) The overexpression efficiency of LINC00520 and the impact of LINC00520 upregulation on FOXP3 expression were determined by RT-qPCR in LUAD cells. (C) Subcellular localization of LINC00520 was confirmed with subcellular fractionation assay in LUAD cells. (D) Venn pattern showed three putative shared miRNAs for LINC00520 and FOXP3 with online tool DIANA

and miRDB. (E) RT-qPCR was conducted to verify putative miRNA expression in LUAD. (F) MiR-3611 levels in LUAD tissues and normal ones was determined via RT-qPCR. (G) The overexpression efficiency of miR-3611 in LUAD cells was tested through RT-qPCR analysis. (H) Binding sequence between miR-3611 and LIN00520 (FOXP3) were respectively predicted through DIANA and TargetScan. (I) Luciferase reporter experiment verified binding ability of miR-3611 and LINC00520 (FOXP3). (J) Binding abundance of miR-3611 and LINC00520 (FOXP3) was further validated by RIP assay. ***p < 0.001.

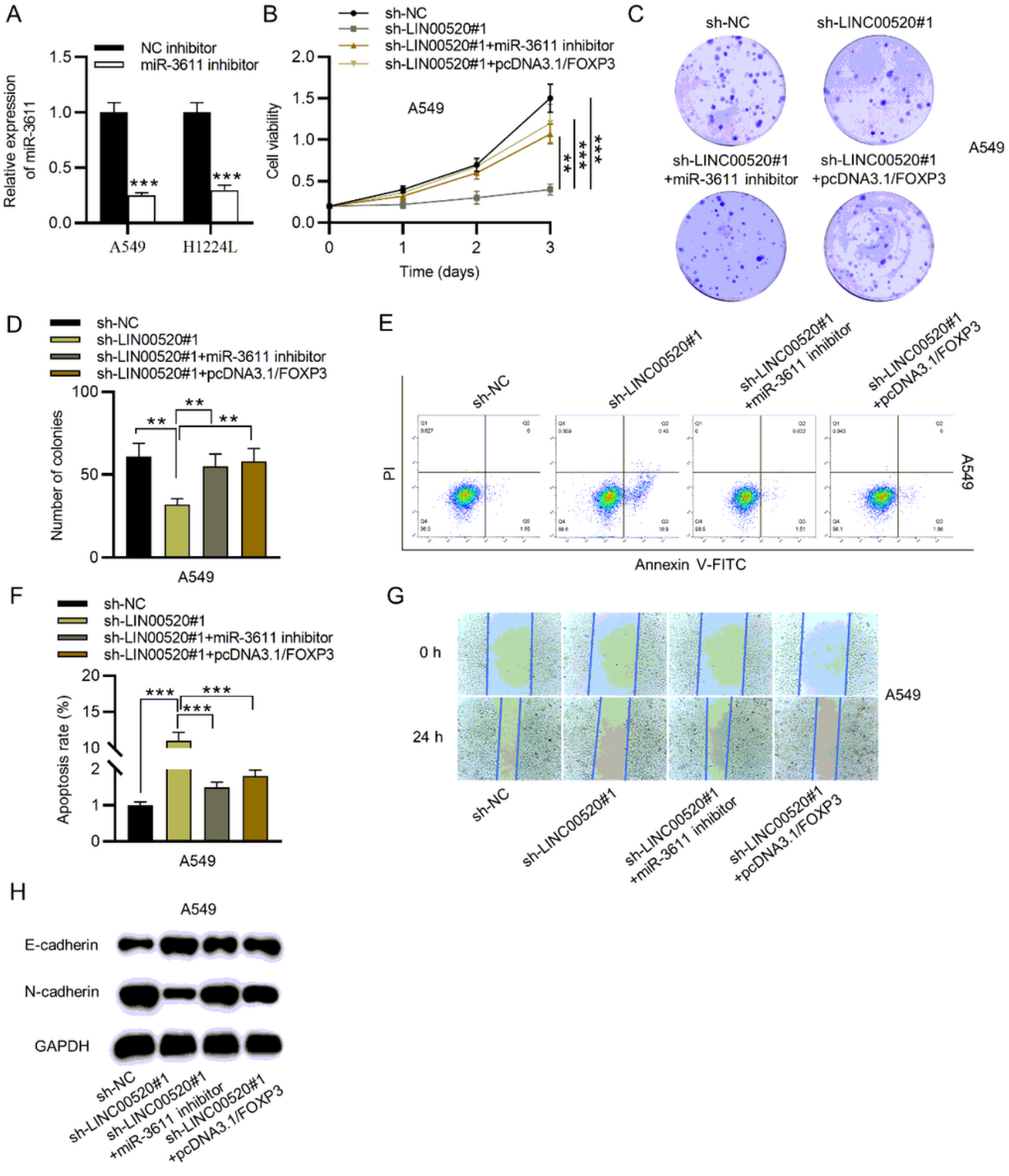

Figure 4

LINC00520 facilitated proliferation and migration in LUAD cells through modulating the LINC00520/miR-3611/FOXP3 axis. (A) Downregulation efficiency of miR-3611 in LUAD cells was measured through RT-qPCR. (B) Cell viability under indicated transfection was confirmed via CCK-8 assay in LUAD. (C-D) Colony formation assay was performed to assure LUAD cell proliferative ability in indicated transfection groups. (E-F) Cell apoptosis in each group in LUAD was validated by flow cytometric analysis. (G) Wound healing assay determined migration of LUAD cells after indicated transfection. (H) Western blot measured protein expression of EMT markers under co-transfection in LUAD. **p < 0.01, ***p < 0.001.

Supplementary Files

This is a list of supplementary files associated with this preprint. Click to download.

- westernblots.pdf